University of Sistan and Baluchestan

Challenges in Nano and Micro Scale Science and Technology

Online ISSN: 2821 - 000X

Structural and Optical Properties Investigations of Pristine and Strontium-Doped Zinc Oxide Synthesized via Pulse Laser Deposition

Ahmad Kamalianfar[1]✉ | Mahmoud Naseri[2]

1. Corresponding Author, Department of Physics Education, Farhangian University, P.O. Box 14665-889, Tehran, Iran. Email: kamalianfar.ahmad@gmail.com
2. Department of Physics, Faculty of Science, Malayer University, Malayer, Iran.

Article Info

Article type:
Research Article

Keywords:
Strontium doped Zinc oxide,
Strontium,
Pulse laser Deposition,
Optoelectronic.

ABSTRACT

Undoped and Strontium doped ZnO thin films were deposited by pulse laser deposition whose average crystallite size lies within the range of 38–53 nm. The deposited film's structure showed that the films crystallized in hexagonal wurtzite structure. The band gap was originating to be 3.31 and 3.20 eV for undoped ZnO and Sr doped ZnO thin films, respectively due to the lattice distortion and creation of active imperfections in the ZnO lattice. The photoluminescence emissions confirmed the presence of defects related to oxygen vacancies and zinc interstitials. SEM images revealed plate-like morphology with hexagonal shape regardless of the sizes. The sensing results revealed that ZnO doped 3% Strontium exhibited the highest response, achieving 41 % at 50 ppm ethanol at an operating temperature of 352℃. The electrical sheet resistance per square area of undoped ZnO and Sr doped ZnO thin films was obtained to be $4.5 \times 10^{+7} \frac{\Omega}{sq}$ and $7.0 \times 10^{+7} \frac{\Omega}{sq}$, respectively. ZnO thin films have been studied extensively for electronics and optoelectronic applications.

INRODUCTION

Due to its high potential utility in various applications, such as electronics, optoelectronics and photonic, ZnO is recognized as one of the most attractive semiconductors. ZnO has direct wide band gap (band gap energy = 3.37 eV) and large exciton binding energy of 60 meV.

ZnO is considered as a potentially attractive material due it's excellent oxidation capacity, low toxicity and with good physical and chemical properties.

However, ZnO suffers from disadvantages like absorption of visible light and low electrical conductivity which limit its uses in some fields such as optoelectronics. An effective strategy to overcome them is the doping process [1]. Appropriate doping of ZnO with special impurities and synthesis techniques could potentially create a material with the required parameters.

Several studies have demonstrated the role of different dopants on the physical properties of ZnO thin films. For example, Pramod Agale et al. synthesized Sr doped ZnO via a hydrothermal method. They reported that the highest degradation rate constant of 0.0389 min^{-1} for the 5 % Sr-doped ZnO sample [2]. Muhammad Shahid Nadeem et al. fabricated Sr-doped ZnO thin films through a sol-gel route on a silicon substrate (100) [3]. They reported that with increasing Sr content, the crystalline superiority is enhanced. Alqa Saeeda Javaid et al. synthesized Strontium doped ZnO nanoparticles and Studied set out to quantify the impact of Strontium doping in Zinc Oxide on various properties [4]. It has been found that how Sr doping affects ZnO films is controversial and debatable [5, 6].

Thus, we report the growth of ZnO thin film with Sr doping on silicon substrate using pulse laser deposition and present results of measurements of optical and electrical properties.

MATERIALS AND METHODS

Sr doped ZnO was deposited on silicon (100) substrate by pulsed laser deposition. We have used Sr doped ZnO (3 wt.%) sintered pellet as PLD target.

A schematic diagram of the pulsed laser deposition setup is shown in Fig.1. To prepare the target, 3 wt% of strontium nitrate nano-hydrate (Sr $(NO_3)_2.9H_2O$) was individually dissolved in an aqueous solution of 0.4 M zinc acetate hexahydrate ($Zn(NO_3)_2.6H_2O$) and agitated for 100 min. Then, citric acid was used as a product stabilizer to form a clear and homogenous solution. In the filtration step, the precipitate was separated from solution by filtration. Later, it was washed with deionized water and

How to Cite this paper: Kamalianfar A., Naseri M. Structural and Optical Properties Investigations of Pristine and Strontium-Doped Zinc Oxide Synthesized via Pulse Laser Deposition. *Challenges in Nano and Micro Scale Science and Technology*. 2023; 11(2): 27-32. DOI: 10.22111/cnmst.2025.50508.1256

Publisher: University of Sistan and Baluchestan.

DOI: 10.22111/cnmst.2025.50508.1256

ethanol, then dried at 80 °C for 4 h and finally calcined at 550 °C for five hours. Finally, pellets of this material is obtained by pressing the produced powder with a hydraulic press at 5 MPa. A sintering process (at 600 °C for 2 hours) was used to make pellets more compact.

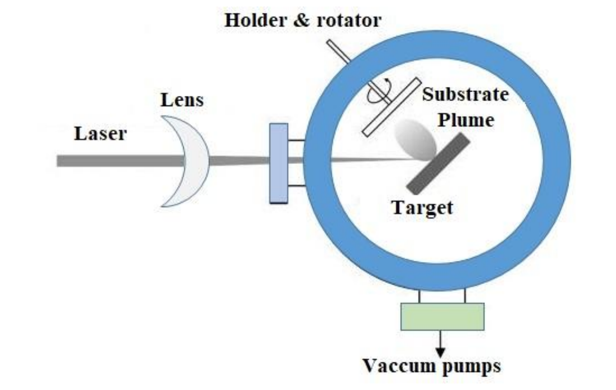

Fig. 1. A schematic diagram of the pulsed laser deposition setup

RESULTS AND DISCUSSION

Structural Analysis

The XRD patterns of pristine ZnO and 3 at% Sr doped ZnO samples are presented in Fig. 2a.

All the observed diffraction peak can be indexed to wurtzite ZnO structure, and no diffraction peaks from Sr or other impurities are detected in the spectrum. The broad diffraction peaks of Sr doped ZnO sample suggests that as the Sr ion is doped, the crystalline size decreases. The observation of a small shift in some peaks to lower angles confirms that Sr ions occupy the Zn sites into the crystal lattice of ZnO (Fig. 2b) [7].

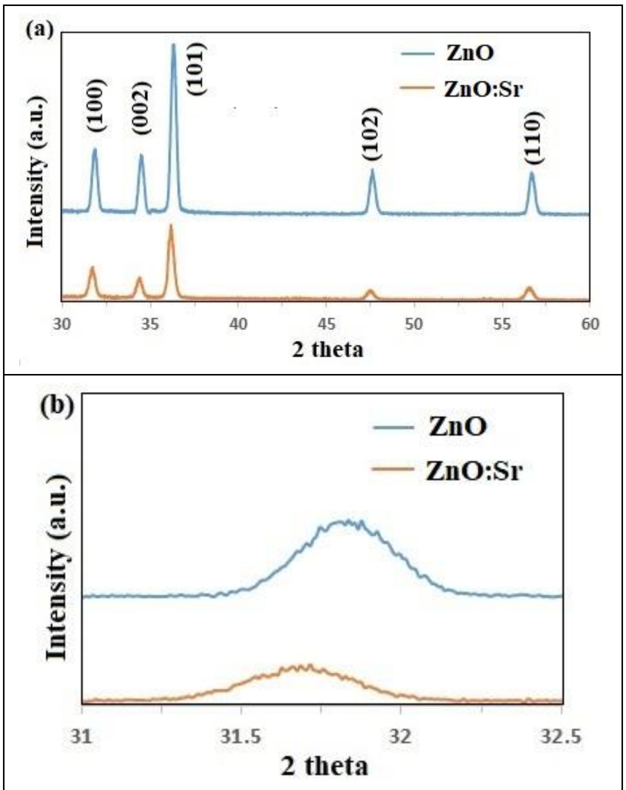

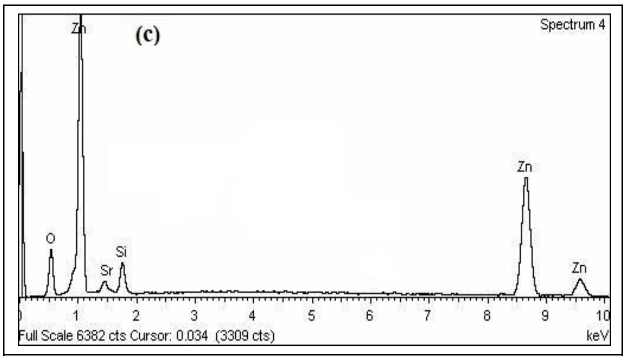

Fig. 2. (a) XRD patterns of pristine ZnO, ZnO:Sr 3% thin films, **(b)** Peak shifting of (100) plane, **(c)** EDS spectrum of ZnO:Sr 3%

According to the composition analysis (Fig. 1c) using EDS measurement, the peaks of Zn, O, Si and Sr elements are observed in the Sr doped ZnO film. The Williamson–Hall (W-H) based X-ray peak analysis method was employed to evaluate the average crystallite size and lattice strain from the XRD peak broadening analysis.

The formula for the W-H method is as [8]:

$$\beta \cos(\theta) = \frac{k\lambda}{D} + 4\varepsilon \sin(\theta) \qquad (1)$$

This formula incorporates a shape factor (k) of 0.94, the wavelength of X-ray source ($\lambda = 1.5405$ Å), the diffraction angle (θ), the micro-strain in the crystal lattice (ε), and the full-width at half maxima (FWHM) of the diffraction line (β). The crystallite size and lattice strain in the samples can be determined from the intercept and strain from slope line plotted between $4\sin(\theta)$ on the X-axis and $\beta\cos(\theta)$ on the Y-axis and as shown in Fig. 3.

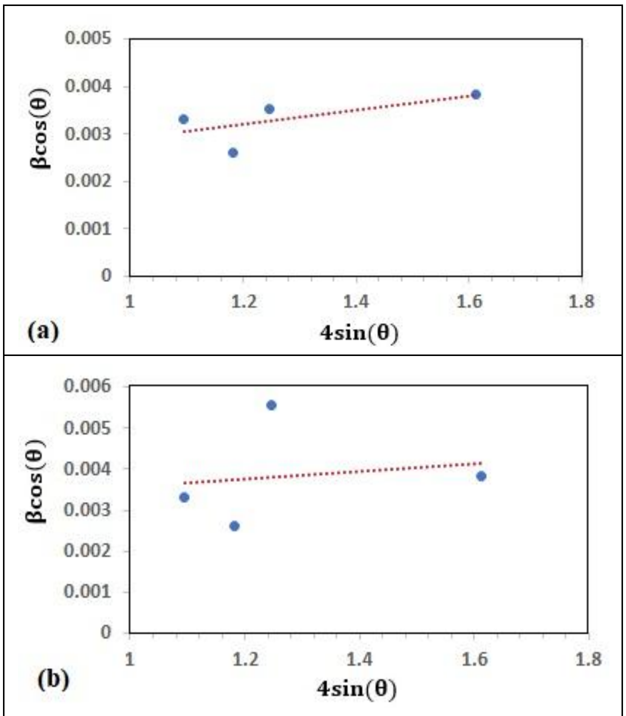

Fig. 3. Linear fit plot of W-H method for calculating crystallite size of (a) pristine ZnO, and (b) ZnO:Sr 3% thin films

The average crystallite sizes calculated from W-H method for the ZnO and 3 at% Sr doped ZnO samples were 53 ± 1 and 38 ± 1 nm, respectively. However, the addition of Sr atoms to the ZnO lattice resulted in an increase in the lattice strain from 1.5×10^{-3} to 2.6×10^{-3}. The crystallite size and other parameters such as lattice strain are listed in Table 1.

Table 1
Structural parameters of pristine ZnO and Sr doped ZnO samples.

Samples	ZnO	Sr doped ZnO
FWHM (101) (°)	0.165	0.323
Lattice parameter (a) (nm)	0.3181	0.3210
Lattice parameter (c) (nm)	0.5031	0.5083
Crystallite Size (nm)	53	38
Lattice Strain ($\times 10^{-3}$)	1.5	2.6

SEM Analysis

The surface morphologies of thin films were monitored by employing scanning electron microscope (SEM, JEOL JSM6490). Fig. 4 shows typical SEM images of Sr doped ZnO thin film which reveals plate-like morphology with a diameter of 1–2 μm and a thickness of 50–150 nm. Most of plates have hexagonal shape regardless of the sizes. The SEM results indicated that no significant morphology change was observed between Sr doped and undoped ZnO thin films. In addition, some random agglomeration of ZnO particles was observed on the surface morphology of thin films due to the strong surface energy [9] or the factors governing the film thickness [10].

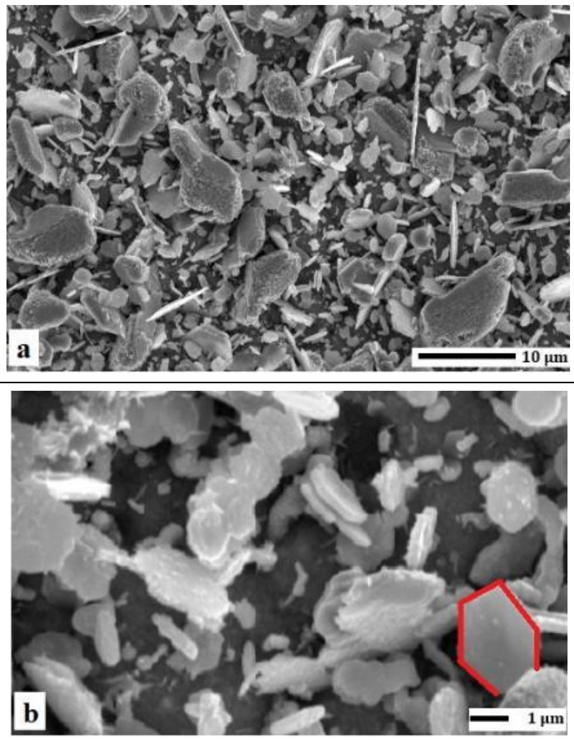

Fig. 4. SEM image of 3% Sr doped ZnO

UV–vis Analysis

Optical absorption behaviour of the thin films is studied from the room temperature UV-Vis spectra in the range of 350-550 nm. Fig. 5. shows the comparison of the absorption spectra of undoped and Sr doped ZnO samples. The results show that ZnO and Sr doped ZnO absorption bands were detected in the UV region at 366 nm and 372 nm, respectively.

The band gap Eg of the samples the prepared samples were estimated according to Tauc's equation [11]:

$$(\alpha h\nu)^{\frac{1}{m}} = A(h\nu - E_g) \qquad (2)$$

Where hv is incident photon energy, α is absorption coefficient, A is a constant, m equals 1/2, 2, 3/2 and 3 for direct allowed, indirect allowed, direct forbidden and indirect forbidden transitions, respectively, and E_g is band gap energy. The band gap of undoped and Sr doped ZnO samples calculated from UV-VIS study was. 3.31eV and 3.20 eV, respectively the experiment revealed that the Sr doping decreased the optical band gap. A literature review on the influence of Sr doping on the band gap of ZnO is given in Table 2.

Table 2
Literature review of the effect of Sr-doping on the band gap of ZnO.

Sample	Sr-doped ZnO hexagonal nanodisks	Sr-doped ZnO thin films	Sr-doped ZnO	Sr doped ZnO thin film
Method of preparation	hydrothermal	sol-gel dip coating	simple wet chemistry route	PLD
Percentage of Sr doping	0-8 %	1, 2 %	0- 3 %	3%
Values of Eg (eV)	Reduction (3.13–2.87)	Reduction (3.28—3.20)	Reduction (3.27 – 2.98)	Reduction (3.31—3.20)
Reference	[2]	[3]	[4]	This work

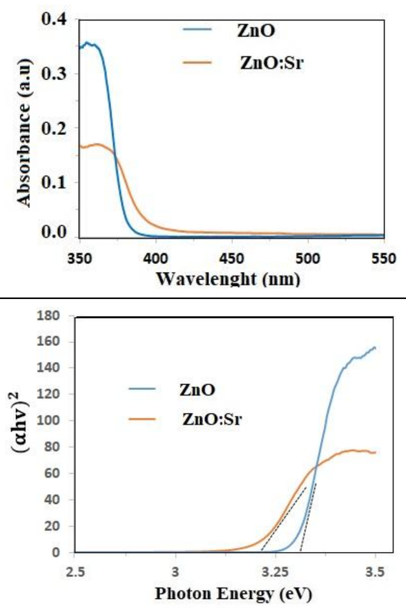

Fig. 5. UV-Vis spectra of ZnO and ZnO:Sr 3% thin films

Photoluminescence Analysis

The characteristic emission spectrum can be used to identify the impurity levels through PL emission. The photoluminescence spectra analysis (Fig. 6) showed two main emission peaks; a strong broad UV emission peak corresponds to a near band edge UV emission, and another a broad defect related emission peak.

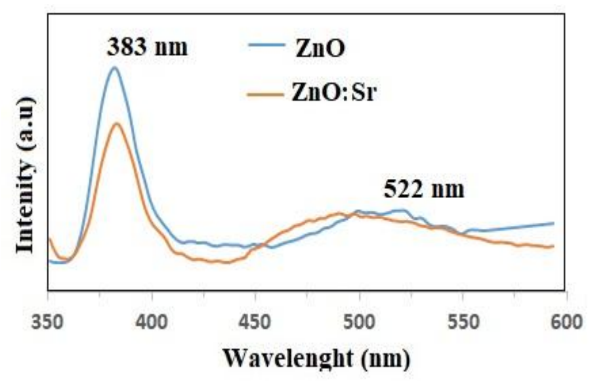

Fig. 6. Room-temperature PL spectra of ZnO and ZnO:Sr 3% thin films

The UV emission peak at 383 nm is attributed to the recombination of free excitons and the broad visible emission band located at 500–550 nm is due to the presence of defects, intrinsic defects like oxygen vacancies and zinc interstitials [12]. The results demonstrate that with incorporation of strontium in ZnO matrix, the intensity of the NBE emission peak gradually decreases, although the intensity of the DLE peaks shows opposite trend. This shows that the doping of Sr atom in the ZnO structure increases the probability of vacancy and/or impurity concentration [13].

From the PL spectra, the intensity ratio of the near-band edge emission to the deep-level emission decreased from 6 for ZnO to 3 for ZnO:Sr thin films, indicating enhanced charge carrier separation and reduced the recombination of the photo-induced electron and hole pair when Sr is doped into the ZnO structure, thereby enhancing photocatalytic performance [14]. The electrical conductivity of thin films can be affected by various factors, including doping [15].

Electrical Properties

A four-point probe (also known as the Kelvin technique) is usually used for measuring thin film resistances. The natural log of resistivity profiles of pristine and Sr doped ZnO thin films as a function of the inverse of the temperature are illustrated in Fig. 7. An approximate linearly decrease of resistivity is observed with rising temperature, indicating the semiconducting behavior of the thin film, because the increased thermal energy allows more electrons to be excited to conduction band across the band gap. As a result, the electrical resistivity decreases with rising the conductivity value in thin films.

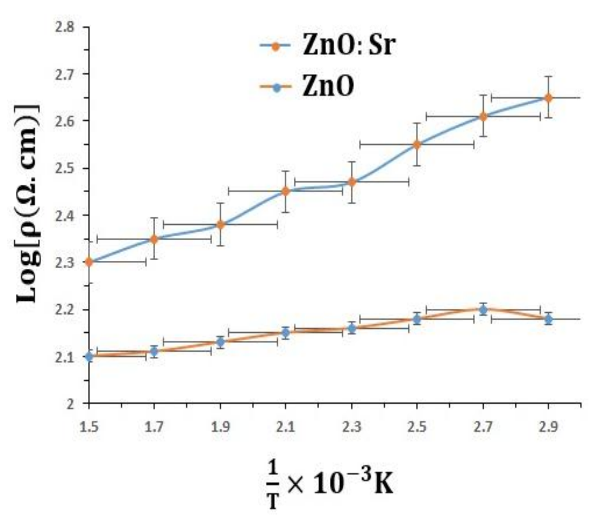

Fig. 7. Logarithmic temperature dependence of resistivity with error bars

The obtained result from the electrical resistivity measurement noticed that after Sr doping, the electrical resistivity of ZnO film is decreased by nearly two orders of decade. Based on the free electron model, the incorporation of Sr in ZnO lattice leads to an increasing in free electrons concentration and to a decrease in films resistivity [16]. The electrical sheet resistance of thin films can be obtained from $Rs = \rho/t$, where, ρ is the electrical resistivity in Ω cm and t is the thickness of the film in meter [17].

A measure of lateral resistance per square area of the films with about 200 nm thickness was calculated. The Electrical parameters of ZnO and Sr doped ZnO thin films at 352 K are listed in Table 3.

Table 3
Electrical parameters of ZnO and Sr doped ZnO thin films at 352 K.

Sample	ρ (Ω. cm) 352K	$R_s\left(\frac{\Omega}{sq}\right)$ 352K	Gas response (%) to 400 ppm ethanol at 352 K
ZnO	8.93	$4.5 \times 10^{+7}$	~11
Sr doped ZnO	14.01	$7.0 \times 10^{+7}$	~41

Interaction between gas molecules and a metal oxide surface provides an electrical signal based on the adsorption or desorption of gases according to the change of resistance. When a metal oxide is exposed to a specific gas molecule, for example ethanol, the electric current of the metal oxide changes. Therefore, as an electrical characteristic of our samples, the change in the conductivity upon exposure to ethanol (400 ppm) is investigated.

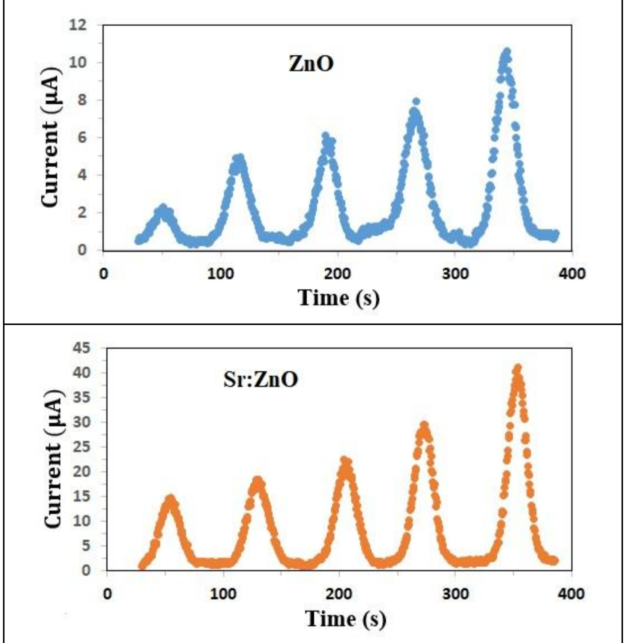

Fig. 8. The ethanol gas response of ZnO and ZnO:Sr 3% thin films

Gas response value can be defined by $(I_g - I_a)/I_a$, where Ig is the sensor current value under ethanol, and Ia is the current value under air. Fig. 8 depicts the gas sensing performance of the synthesized thin films. The Sr doped ZnO thin film shows a remarkably high sensing response as compared to the undoped ZnO film because it is known that various dopant incorporation (here Sr doping) increases number of free charge carriers and facilitates gas sensing process [18,19].

CONCLUSION

In summary, Sr doped ZnO thin film prepared by PLD was successfully deposited on Si (100) substrate. The films were then characterized and studied for their morphology, structure, optical parameters. The SEM shows the construction of hexagonal shape particles. The Photoluminescence study indicated that the Sr content reduces oxygen vacancies and suppress non-radiative recombination. The intensity ratio of the UV emission to the DL emission, indicating enhanced charge carrier separation. Sr doped ZnO displayed significantly enhanced sensing response (about 41% at 352 °C) toward 400 ppm of ethanol gas compared to undoped ZnO sensor. The results showed that Sr doped ZnO thin film may be useful for some optoelectronic applications.

CONFLICT OF INTEREST

The authors declare no competing interests.

REFERENCES

[1] Abdel-Latif MK, Mobarak M, Revaprasadu N, Ashraf AH, Othman W, Khalefa MM, Aboud AA, Ismail M. Effect of doping on the structural, optical and electrical properties of La-doped ZnO thin films. Journal of Materials Science: Materials in Electronics. 2023 Feb;34(4):254.

[2] Agale P, Salve V, Mardikar S, Patange S, More P. Synthesis and characterization of hierarchical Sr-doped ZnO hexagonal nanodisks as an efficient photocatalyst for the degradation of methylene blue dye under sunlight irradiation. Applied Surface Science. 2024 Nov 1;672:160795.

[3] Nadeem MS, Baoji M, Alam MM, Riaz NN, Al-Sehemi AG, Munawar T, Mukhtar F, Rabbani AW, Naz A, Al-Tahan MA, Iqbal F. Sr-doped ZnO thin film on a silicon substrate (100) grown by sol-gel method: Structural and optical study. Optical Materials. 2024 Nov 1;157:116106.

[4] Javaid AS, Javaid WS, Adnan M, Usman M, Akram MA, Bashir N, Khalid A, Ahmad P, Hossin MM, Liaqat I, Ismail MA. Synthesis and characterization of efficient Sr-doped ZnO nanostructures for optoelectronic, and photocatalytic applications. Inorganic Chemistry Communications. 2024 Apr 1;162:112175.

[5] Yarahmadi M, Maleki-Ghaleh H, Mehr ME, Dargahi Z, Rasouli F, Siadati MH. Synthesis and characterization of Sr-doped ZnO nanoparticles for photocatalytic applications. Journal of Alloys and Compounds. 2021 Feb 5;853:157000.

[6] Mansouri I, Saib F, Boulahlib S, Laachachi A, Özacar M, Bessekhouad Y. Effect of Sr-doping toward the optoelectrical ZnO properties. Inorganic Chemistry Communications. 2024 Apr 1;162:112236.

[7] Altowyan AS, Çoban MB, Kaynar UH, Hakami J, Çin EA, Kaynar SC, Ayvacikli M, Can N. Lattice distortion effects induced by Li+ co-doping on ZnO: Tb3+ phosphors: Photoluminescence and unusual hypersensitive $^5D_4 \rightarrow$ $^7F_0$ transition. Ceramics International. 2024 Jul 1;50(13):24036-44.

[8] Bouderbala IY, Guessoum A, Rabhi S, Bouhlassa O, Bouras IE. Optical band-diagram, Urbach energy tails associated with photoluminescence emission in defected ZnO thin films deposited by sol–gel process dip-coating: effect of precursor concentration. Applied Physics A. 2024 Mar;130(3):205.

[9] Khan SA, Rahman A, Ibrahim FB. The impact of film thickness on the properties of ZnO/PVA nanocomposite film. Materials Research Express. 2021 Jul 2;8(7):075002.

[10] Haryński Ł, Olejnik A, Grochowska K, Siuzdak K. A facile method for Tauc exponent and corresponding electronic transitions determination in semiconductors directly from UV–Vis spectroscopy data. Optical Materials. 2022 May 1;127:112205.

[11] Rahmanifar E, Azarang M, Aliahmad M. Efficient photodegradation of Rhodamine B dye assisted by Pigskin-Gel via sustainable synthesis of Fe2O3@ rGO nanocrystals with magnetically separable properties. Journal of Sol-Gel Science and Technology. 2024 Sep;111(3):671-88.

[12] Algün G, Akçay N, Öztel HO, Can MM. Synthesis and ultrafast humidity sensing performance of Sr doped ZnO nanostructured thin films: the effect of Sr concentration. Journal of Sol-Gel Science and Technology. 2023 Sep;107(3):640-58.

[13] Siebenhofer M, Viernstein A, Morgenbesser M, Fleig J, Kubicek M. Photoinduced electronic and ionic effects in strontium titanate. Mater. Adv. 2 (23), 7583–7619 (2021) [Internet].

[14] Basseem M, Emam AA, Kamal FH, Gamal AM, Abo Faraha SA. Novel functionalized of ZnO with Sm3+, La3+, and Sr2+/ZnO single and tri-doped nanomaterials for photocatalytic degradation: synthesis, DFT, kinetics. Journal of Materials Science. 2023 Sep;58(33):13346-72.

[15] Al Farsi B, Souier TM, Al Marzouqi F, Al Maashani M, Bououdina M, Widatallah HM, Al Abri M. Structural and optical properties of visible active photocatalytic Al doped ZnO nanostructured thin films prepared by dip coating. Optical Materials. 2021 Mar 1;113:110868.

[16] Battal W, Rouchdi M, Shaili H, Ouafi M, Essajai R, Belafhaili A, Hassanain N, Mzerd A. Strontium doping effect on characteristics of ultrasonically sprayed zinc oxide thin films. Applied Physics A. 2020 Jul;126:1-0.

[17] Cisneros-Contreras IR, López-Ganem G, Sánchez-Dena O, Wong YH, Pérez-Martínez AL, Rodríguez-Gómez A. Al-doped ZnO thin films with 80% average transmittance and 32 Ohms per square sheet resistance: A genuine alternative to commercial high-performance indium tin oxide. Physics. 2023 Jan 6;5(1):45-58.

[18] Ravikumar P, Mohan R, Gayathri K, Babu BM, Ravichandran K, Devendran P, Vadivel S. Effective NH3 gas sensing at low ppm by ZnO films through improved charge carrier and adsorption: Single and dual doping with Al and Cu-a comparative study. Materials Science and Engineering: B. 2024 Oct 1;308:117558.

[19] Sebastian S, Raj CS, Diana P, Ganesh V, Awwad NS, Yahia IS, AlAbdulaal TH. Rare earth elements terbium (Tb), erbium (Er), ytterbium (Yb) doped zinc oxide nanoparticles: Synthesis structural optical and gas sensing studies. Physica B: Condensed Matter. 2024 Dec 1;694:416384.